Medicinal Chemistry Research (2020) 29:189–198
https://doi.org/10.1007/s00044-019-02472-9

MEDICINAL CHEMISTRY RESEARCH

ORIGINAL RESEARCH

Structural modification of ellipticine derivatives with alkyl groups of varying length is influential on their effects on human DNA topoisomerase II: a combined experimental and computational study

M. Kuskucu[1] · V. Akyildiz[2] · Á. Kulmány[3] · Y. Ergün[2] · S. Zencir[4] · I. Zupko[3] · S. Durdagi[5] · M. Zaka[5] · K. Sahin[5] · H. Orhan[6] · Z. Topcu[1]

Received: 3 June 2019 / Accepted: 6 November 2019 / Published online: 20 November 2019

Abstract

The compounds reducing tumor cell viability and disrupting DNA topoisomerase reactions have been widely used in anticancer drug development. Ellipticine (5,11-dimethyl-6H-pyrido[4,3-b]carbazole) is a potent intercalating agent that interferes with nucleic acid processing through interaction with DNA topoisomerase II. Although ellipticine is a well-characterized compound, it is not a widely-accepted drug due to the adverse effects detected upon administration. We have previously reported two novel ellipticine derivatives, N-methyl-5-demethyl ellipticine (ET-1) and 2-methyl-N-methyl-5-demethyl ellipticinium iodide (ET-2) as potent compounds targeting DNA topoisomerase II. This study covers an extended synthesis, characterization, and activity data for five new salts of N-methyl 5-demetyl ellipticine (Z-1, Z-2, Z-4, Z-5 and Z-6) having several organic halides and their effects on human topoisomerase II enzymes. Moreover, combined in silico studies were conducted for better understanding of modes of action of studied molecules at the binding pocket of target. Our results showed that three of the derivatives (Z-1, Z-2, and Z-6) have considerable effect on the catalytic activity of human topoisomerase II implying the influence of alkyl groups added to the parental structure of ellipticine.

Keywords DNA topoisomerase II · Ellipticine derivatives · Anticancer drugs

Introduction

DNA topoisomerases play fundamental roles in overcoming topological problems of DNA by introducing transient breaks in the duplex during replication, transcription, recombination, and chromosomal segregation (Wang 1971). Given that the inherent functions of topoisomerases are crucial for genomic integrity, the interfere with these enzymes or generating enzyme-mediated DNA damage is an effective strategy in development of chemotherapeutic agents (Coban et al. 2008; Gul et al. 2009; Senarisoy et al. 2013; Ashley and Osheroff 2014; Ketron and Osheroff 2014; Zupkó et al. 2014; Vann et al. 2016a, 2016b; Delgado et al. 2018).

Topoisomerase targeting agents act primarily in two ways: Topoisomerase poisons stabilize the transient phosphotyrosine covalent bond between the enzyme–DNA complexes and kill the cells by increasing the levels of truncated-DNA covalent intermediates (Champoux 2001; Topcu 2001). Alternatively, topoisomerase inhibitors act by disrupting the essential catalytic functions of the enzymes. It

Supplementary information The online version of this article (https://doi.org/10.1007/s00044-019-02472-9) contains supplementary material, which is available to authorized users.

✉ Z. Topcu
zeki.topcu@ege.edu.tr

[1] Department of Pharmaceutical Biotechnology, Faculty of Pharmacy, Ege University, Izmir 35100, Turkey

[2] Department of Chemistry, Faculty of Science, Dokuz Eylul University, Izmir 35160, Turkey

[3] Institute of Pharmacodynamics and Biopharmacy, Faculty of Pharmacy, University of Szeged, Szeged 6720, Hungary

[4] Department of Medical Biology, Faculty of Medicine, Pamukkale University, Denizli 20070, Turkey

[5] Computational Biology and Molecular Simulations Laboratory, Department of Biophysics, School of Medicine, Bahcesehir University, Istanbul 34734, Turkey

[6] Department of Pharmaceutical Toxicology, Faculty of Pharmacy, Ege University, Izmir 35100, Turkey

has also been shown that catalytic inhibitors affect various stages of the catalytic cycle of topoisomerase II, including the cleavage of DNA while some compounds manifest both DNA breakage patterns as well as enzyme inhibition (Topcu 2001).

The natural product ellipticine (5,11-dimethyl-6H-pyrido-[4,3-b]carbazole) is one of the carbazole alkaloids with a potent anticancer activity. Several key mechanisms of action, including DNA intercalation and topoisomerase II inhibition, bio-oxidation, adduct formation, mitochondrial membrane modulation, inhibition of p53 and interaction with kinases such as c-Kit and AKT contribute to the anticancer activity of ellipticine (Vann et al. 2016b; Garbett and Graves 2004; Kuo et al. 2005; Thompson et al. 2008; Chikamori et al. 2010). Like several other topoisomerase-targeting drugs, a number of adverse side effects such as xerostomia, weight loss, hemolysis, and renal toxicity are also associated with ellipticine administration mostly due to its cytochrome P450 (CYP)- and/or peroxidase-mediated activation yielding covalent DNA adducts (Rouëssé et al. 1993; Lichota and Gwozdzinski 2018). Therefore, over the last years, obtaining new natural or synthetic derivatives to replace the known topoisomerase-targeting compounds gained a significant attention.

Several derivatives of ellipticine have been investigated (Moody et al. 2007; Miller et al. 2012; Deane et al. 2013; Iacopetta et al. 2017). We previously reported two novel ellipticine derivatives, N-methyl-5-demethyl ellipticine and 2-methyl-N-methyl-5-demethyl ellipticinium iodide that both were potent topoisomerase II-targeting compounds (Vann et al. 2016b). We now synthesized and characterized five new derivatives of ellipticine having alkyl groups of different lengths with increased carbon number (Z-1 and Z-2) and substituted alkyl groups (cyanoalkyl) (Z-4 and Z-5) as well as a derivative with an inserted amide alkyl group (Z-6). We monitored their effect on tumor cell growth and human topoisomerase II activities and also conducted in silico studies.

Materials and methods

Chemistry

We investigated side chain substituent effect at the N-2 position in order to increase the solubility and activity of the compounds. The salts of N-methyl 5-demetyl ellipticine were synthesized using N-methyl 5-demetyl ellipticine and several alkyl halides, cyano alkyl halides, and amide alkyl halide (Fig. 1). Melting points were measured in sealed tubes using an electro thermal digital melting point apparatus (Gallenkamp, London, UK). Fourier transform infrared spectroscopy (FTIR) analyses using PerkinElmer Spectrum BX-II Model FTIR spectrophotometer were carried out for characterization of synthesized molecules. The samples within KBr pellets were measured in the range of 4000–400 cm^{-1}. ^{1}H-NMR and ^{13}C-NMR spectra were obtained on a Varian AS-400 NMR spectrometer with tetramethylsilane as an internal standard (Oxon, UK).

Synthesis of N^2-methyl N-methyl 5-demethyl ellipticine salts

N-Methyl 5-demethyl-ellipticine (2 mmol) was suspended in dimethylformamide (5 mL), and organic halide (2.2 mmol) was added (Vann et al. 2016b). The reaction mixture was stirred at room temperature for 5 h, quenched with cold ether (5 mL), and the resulting precipitate was collected with vacuum filtration. The precipitate was washed with cold ethanol (2.5 mL) to yield N-methyl 5-demethyl ellipticine salts (Z-1, Z-2, Z-4, Z-5, Z-6) (Fig. 1).

N^2-Ethyl N-methyl 5-demethyl ellipticinium bromide (Z-1)

Yield: 45%; mp: 296 °C; IR (KBr) ν_{max}: 3020 (CH), 2974 (CH), 1619 (C=N) cm^{-1}; ^{1}H-NMR (DMSO-d_6, 400 MHz): δ 1.60 (t, 3H, $^{+}NCH_2CH_3$), 2.97 (s, 3H, CH_3), 3.74 (s, 3H, NCH_3), 4.67 (q, 2H, $^{+}NCH_2CH_3$), 7.25 (t, 1H, $J = 7.6$ Hz, ArH), 7.43 (d, 1H, $J = 7.6$ Hz, ArH), 7.52 (d, 1H, $J = 7.2$ Hz, ArH), 7.73 (s, 1H, ArH), 8.09 (d, 1H, $J = 7.6$ Hz, ArH), 8.13 (d, 1H, $J = 6.4$ Hz, ArH), 8.36 (d, 1H, $J = 6.4$ Hz, ArH), 9.82 (s, 1H, ArH); ^{13}C-NMR (DMSO-d_6, 100 MHz): 15.22, 16.89, 29.58, 55.74, 101.41, 109.82, 119.83, 121.34, 121.35, 124.17, 124.24, 125.55, 128.97, 131.17, 134.75, 135.05, 143.21, 145.38, 145.77.

N^2-Hexyl N-methyl 5-demethyl ellipticinium bromide (Z-2)

Yield: 52%; mp: 132 °C; IR (KBr) ν_{max}: 3047 (CH), 2929 (CH), 1622 (C=N) cm^{-1}; ^{1}H-NMR (DMSO-d_6, 400 MHz): δ 0.85 (t, 3H, $J = 7.2$ Hz, CH_3), 1.24–1.45 (m, 6H, 3xCH_2), 1.96–2.08 (m, 2H, CH_2), 3.17 (s, 3H, CH_3), 3.85 (s, 3H, NCH_3), 4.67 (t, 2H, $J = 7.6$ Hz, $^{+}NCH_2$), 7.35 (t, 1H, J = 7.6 Hz, ArH), 7.61–7.69 (m, 2H, ArH), 7.96 (s, 1H, ArH), 8.27 (d, 1H, $J = 6.8$ Hz, ArH), 8.31 (d, 1H, $J = 8$ Hz, ArH), 8.47 (d, 1H, $J = 6.8$ Hz, ArH), 10.02 (s, 1H, ArH); ^{13}C-NMR (DMSO-d_6, 100 MHz): 14.17, 15.08, 22.27, 25.61, 29.45, 30.96, 31.18, 60.24, 100.82, 109.66, 119.66, 121.13, 121.30, 124.02, 124.09, 125.43, 128.90, 131.31, 134.62, 134.87, 143.02, 145.22, 145.54.

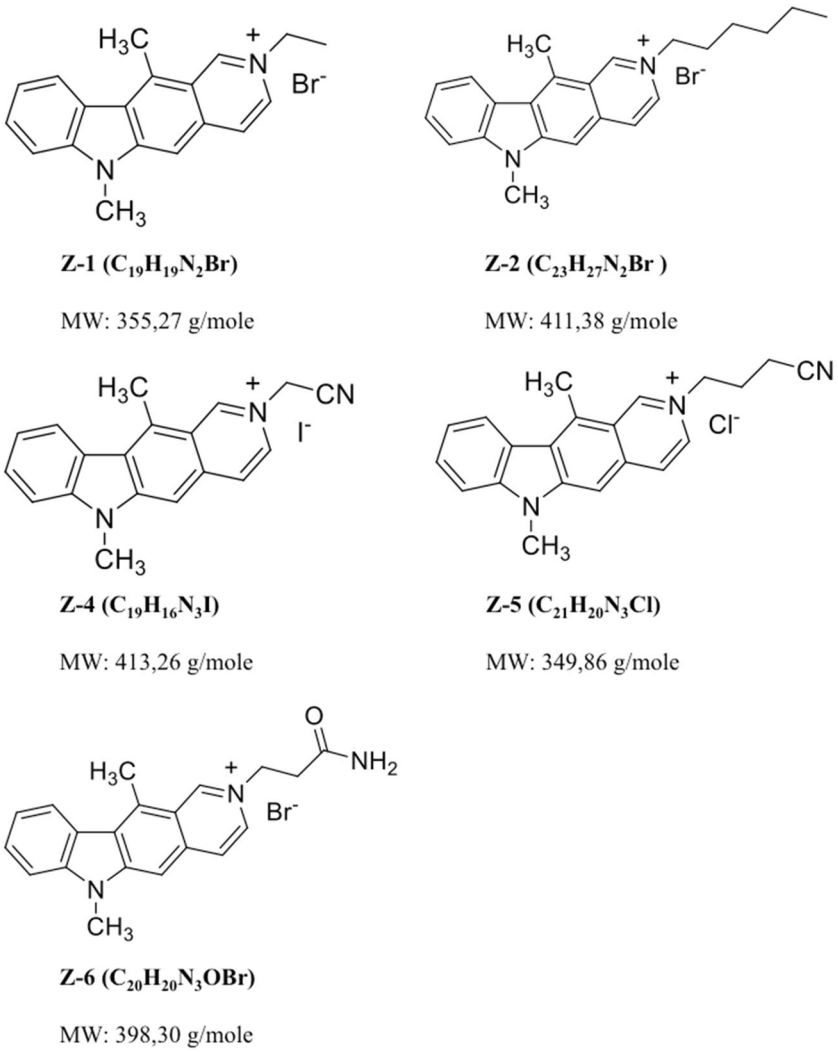

Fig. 1 Ellipticine derivatives covered in this study

N^2-Cyanomethyl N-methyl 5-demethyl ellipticinium iodide (Z-4)

Yield: 28%; mp: 189 °C; IR (KBr) ν_{max}: 3042 (CH), 2924 (CH), 2218 (CN), 1619 (C=N) cm^{-1}; ^{1}H-NMR (DMSO-d_6, 400 MHz): δ 3.20 (s, 3H, CH_3), 3.89 (s, 3H, NCH_3), 5.97 (s, 2H, $^+NCH_2CN$), 7.38–7.42 (m, 1H, ArH), 7.62–7.69 (m, 2H, ArH), 8.02 (s, 1H, ArH), 8.36 (d, 2H, $J = 6.8$ Hz, ArH), 8.51 (d, 1H, $J = 6.8$ Hz, ArH), 10.10 (s, 1H, ArH); ^{13}C-NMR (DMSO-d_6, 100 MHz): 14.09, 29.87, 62.41, 100.81, 109.52, 119.67, 120.08, 121.14, 121.32, 123.45, 124.09, 125.41, 128.87, 131.37, 134.76, 135.11, 142.97, 145.28, 146.27.

N^2-(3-Cyanopropyl) N-methyl 5-demethyl ellipticinium chloride (Z-5)

Yield: 35%; mp: 116 °C; IR (KBr) ν_{max}: 3047 (CH), 2924 (CH), 2246 (CN), 1619 (C=N) cm^{-1}; ^{1}H-NMR (DMSO-d_6, 400 MHz): δ 2.32–2.40 (m, 2H, CH_2), 2.75 (t, 2H, $J =$ 6.8 Hz, CH_2), 2.99 (s, 3H, CH_3), 3.68 (s, 3H, NCH_3), 4.76 (t, 2H, $J = 6.8$ Hz, $^+NCH_2$), 7.25 (t, 1H, $J = 7.2$ Hz, ArH), 7.45 (d, 1H, $J = 8$ Hz, ArH), 7.53 (t, 1H, $J = 8$ Hz, ArH), 7.74 (s, 1H, ArH), 8.10 (d, 1H, $J = 8$ Hz, ArH), 8.16 (d, 1H, $J = 6.8$ Hz, ArH), 8.41 (d, 1H, $J = 6.4$ Hz, ArH), 9.99 (s, 1H, ArH); ^{13}C-NMR (DMSO-d_6, 100 MHz): 14.08, 15.17, 26.79, 29.46, 58.68, 100.85, 109.69, 119.69, 120.16, 121.12, 121.29, 123.56, 124.07, 125.37, 128.86, 131.35, 134.73, 135.09, 142.99, 145.26, 146.25.

N^2-(Carboxyaminoethyl) N-methyl 5-demethyl ellipticinium bromide (Z-6)

Yield: 21%; mp: 119 °C; IR (KBr) ν_{max}: 3058 (CH), 2935 (CH), 1673 (C=O), 1619 (C=N) cm^{-1}; ^{1}H-NMR (DMSO-d_6, 400 MHz): δ 2.76 (t, 2H, $J = 6.8$ Hz, CH_2), 3.20 (s, 3H, CH_3), 3.88 (s, 3H, NCH_3), 4.89 (t, 2H, $J = 6.8$ Hz, $^+NCH_2$), 7.05 (m, 1H, ArH), 7.40 (m, 1H, ArH), 7.56 (m, 1H, ArH), 7.68 (s, 1H, NH_2), 7.99 (m, 1H, ArH), 8.28 (d, 1H, $J =$ 7.6 Hz, ArH), 8.36 (d, 1H, $J = 7.6$ Hz, ArH), 8.46 (d, 1H, J

= 6.4 Hz, ArH), 10.04 (s, 1H, ArH); ^{13}C-NMR (DMSO-d_6, 100 MHz): 15.51, 29.92, 36.31, 56.39, 101.58, 110.32, 120.02, 121.61, 121.82, 123.89, 124.71, 126.09, 129.21, 132.16, 135.18, 135.67, 142.76, 146.02, 147.50, 171.40.

Biology

Materials

pBR322 plazmid DNA, kinetoplast DNA (kDNA), recombinant human topoisomerase II were purchased from Inspiralis (Inspiralis, *Norfolk*, UK). Human cervix adenocarcinoma (HeLa and SiHa) and breast adenocarcinoma (MCF-7 and MDA-MB-231) cancer cell lines were purchased from European Collection of Cell Cultures (Salisbury, UK).

Cell culturing and viability assay

Cells were maintained in minimal essential medium supplemented with 10% fetal bovine serum, 1% non-essential amino acids and an antibiotic–antimycotic mixture (all from Lonza Group Ltd., Basel, Switzerland). The antiproliferative properties of the prepared analogs were determined by means of MTT (3-(4,5-dimethylthiazol-2-yl)-2,5-diphenyltetrazolium bromide, Sigma Aldrich Ltd. (Budapest, Hungary) assay (Mosmann 1983). Briefly, near-confluent cancer cells were seeded onto a 96-well microplate (5000/well) and, after an overnight standing, new medium, containing the tested compounds was added. After incubation for 72 h in humidified air with 5% CO_2 at 37 °C, the viability of the cells were determined by the addition of 44 µL of 5 mg/mL MTT solution. The living cells metabolized the MTT and the produced formazan was precipitated as purple crystals during a 4-h contact period. The medium was next removed and the formazan was dissolved in 100 µL of dimethylsulfoxide (DMSO) during a 60-min period of shaking at 37 °C. Finally, the reduced MTT was assayed at 545 nm (Stat Fax-2100, Awareness Technologies Inc., Palm City, FL, USA), sigmoidal concentration–response curves were fitted to the determined data and the IC_{50} values were calculated by means of GraphPad Prism 4.0 (GraphPad Software, San Diego, CA, USA). All in vitro experiments were carried out on two microplates with five parallel wells. Stock solutions of the tested compounds (10 mM) were prepared in DMSO. The highest DMSO content of the medium (0.3%) did not have any substantial effect on the cell proliferation. Cisplatin (Ebewe Pharma GmbH, Unterach, Austria) was used as a reference agent. The IC_{50} value is defined as the concentration of a compound that gives half-maximal response.

Topoisomerase activity assays

Decatenation assays were carried out as described (Vann et al. 2016a). Reaction mixtures contained 0.2 µg of kinetoplast DNA (kDNA) from *Crithidia fasciculata* and 75 nM and human topoisomerase II alfa in a final volume of 20 µL of 50 mM Tris-Cl, pH 8.0, 120 mM KCl, 10 mM $MgCl_2$, 0.5 mM ATP, and 0.5 mM dithiothreitol. Reactions were carried out in the absence or presence of compounds for 15 min at 37 °C and terminated with 5% sarkosyl, 0.0025% bromophenol blue, and 25% glycerol. Samples were mixed with 2 µL of agarose loading dye (60% sucrose in 10 mM Tris-HCl pH 7.9, 0.5% bromophenol blue, and 0.5% xylene cyanol FF), heated for 2 min at 45 °C and subjected to electrophoresis using 1% agarose gels in 40 mM Tris-borate, pH 8.3 and 2 mM EDTA containing 0.5 µg/mL ethidium bromide (Et-Br). DNA bands were visualized under UV light and average band intensities were calculated from three independent reactions using *GeneSys* program (SynGene, Frederick MD, USA). DNA decatenation was monitored by the conversion of large catenated networks that remained at the origin to decatenated minicircles. One unit of human topoisomerase II was corresponding to decatenation the 200 ng of kDNA substrate for 15 min at 37 °C in the indicated reaction buffer. Supercoil relaxing activity of the enzyme using supercoiled plasmid DNA substrate, pBR322 was also covered for correlation purpose (Topcu et al. 2008).

Cleavage of Plasmid DNA

DNA cleavage assays contained 10 nM negatively supercoiled pBR322 DNA and 150 nM human topoisomerase II of either alfa or beta isoforms in a final volume of 20 µL of 10 mM Tris-HCl, pH 7.9, 5 mM $MgCl_2$, 100 mM KCl, 0.1 mM EDTA, and 2.5% (v/v) glycerol (Senarisoy et al. 2013; Vann et al. 2016a). Mixtures were incubated for 6 min at 37 °C. Enzyme-DNA cleavage complexes were trapped by the addition of 2 µL of 5% SDS followed by 2 µL of 250 mM EDTA, pH 8.0. Proteinase K (2 µL of a 0.8 mg/mL solution) was added, and samples were incubated for 30 min at 45 °C to digest the enzyme. Samples were mixed with 2 µL of agarose loading dye, heated for 2 min at 45 °C and subjected to electrophoresis as above. DNA cleavage was monitored by the conversion of supercoiled plasmid to linear molecules.

DNA intercalation

Human DNA topoisomerase I (0.5 U) and 300 ng of relaxed pBR322 were incubated in 10 mM Tris-HCl, pH 7.5, 10 mM KCl, 2 mM $MgCl_2$, 0.02 mM EDTA, 0.1 mM dithiothreitol, and 6 µg/mL bovine serum albumin in a final

volume of 20 µL (Vann et al. 2016b). Reactions contained either ellipticine derivatives or Et-Br (10 µM), a well-characterized intercalator, used as positive control. Mixtures were incubated for 15 min at 37 °C. Following the addition of 3 µL of stop solution (0.77% SDS 77.5 mM EDTA, pH 8.0), samples were extracted using 20 µL of phenol: chloroform:isoamyl alcohol (25:24:1), and the aqueous layer was mixed with 2 µL of agarose loading dye and heated for 5 min at 45 °C. Intercalation products were subjected to electrophoresis in a 1% agarose gel in 100 mM Tris-borate and 2 mM EDTA. DNA bands were visualized as described above. DNA intercalation was monitored by the conversion of relaxed DNA to supercoiled plasmid populations of different superhelical densities.

In silico simulations

Ligand preparation

The 2D structures of studied ligands were sketched by 2D Sketcher program under Maestro molecular modeling package and prepared by Ligand Preparation module (LigPrep). OPLS3 force field was used to obtain low energy conformers of ligands. Protonation states of ligands were investigated at physiological pH by Epic module. To obtain the lowest energy conformers of ligands, a conformational search method was used in which all possible conformations were generated by a systematic Monte Carlo search algorithm. The effect of slightly higher pH values (i.e., pH 8) to the protonation did not reveal any change.

Protein preparation

The crystal structure of DNA-bound human topoisomerase II alpha was retrieved from Protein Data Bank (PDB ID: 4FM9, 25 (Wendorff et al. 2012)). The protein preparation module of Maestro molecular modeling package was used. The missing side chains of the protein were fixed, protonation states of the amino acids were investigated at the physiological pH 7.4 by PROPKA code. Water molecules within the catalytic domain were kept using protein preparation wizard of Maestro molecular modeling suite. Both backbone and side chain atoms were minimized with OPLS2005 force field to refine the protein.

Molecular docking

Molecular docking studies were performed by Glide and GOLD docking programs (Friesner et al. 2004; Verdonk et al. 2003). The binding interactions were calculated using a genetic algorithm in GOLD. The following steps were applied: (i) a population of potent binding poses at a defined binding pocket is set up at random; (ii) each member of the population is encoded as a "chromosome", which contains information about the mapping of protein−ligand interactions; (iii) each chromosome is assigned a fitness score based on its predicted binding affinity, and the chromosomes within the population are ranked according to fitness; and (iv) the population of chromosomes is iteratively optimized. The following genetic algorithm parameters were used (populations size, 50; selection pressure,1.1; number of islands, 5; migrate, 10; mutate, 95; crossover, 95; niche size, 2; number of operations, 125,000 and search efficiency 200%). The Glide/standard precision (SP), extra precision (XP), induced-fit docking (IFD), and quantum-polarized ligand docking approaches implemented into the Maestro molecular modeling package were also used. The IFD method provides more flexibility to the binding pocket residues. All the ligands were docked into the binding pocket of target using Glide/SP, and then complexes with high docking scores were forwarded to next steps. Amino acids of complexes within the 5 Å of the docked ligands were optimized by Prime module of Maestro. Finally, all ligands were redocked using Glide/XP. In QPLD, initially, Glide/XP docking was carried out to generate ten poses per docked compound. These poses were submitted to QM charge calculations which uses the 6-31G*/LACVP* basis set, B3LYP density functional, and "Ultrafine" SCF accuracy level.

Molecular dynamics (MD) simulations

MD simulations were performed using the Desmond program with the OPLS2005 force field and RESPA integrator (Desmond Molecular Dynamics System 2017). The complex generated from top-docking pose of Glide/SP, was immersed in orthorhombic water box and SPC solvent models were used in the preparation of the system and 0.15 M NaCl salt were added to the box in order to neutralize the used systems. In all MD simulations, NPT ensemble at 310 K with Nose–Hoover temperature coupling (Hoover 1985) and at constant pressure of 1.01 bar via Martyna–Tobias–Klein pressure coupling (Martyna 1994) were used. 2.0 fs time step was used in simulations and 10-ns MD simulations were performed both for selected molecule Z-1 and positive control.

MetaCore/MetaDrug binary QSAR models

MetaDrug uses the property of *Tanimoto Prioritization* to find the similarity between analyzed compounds and compound sets in the quantitative structure–activity relationships (QSAR) models based on elements found in the structure (Metacore/Metadrug platform, Clarivate Analytics 2019). These models were prepared with a diverse set of compounds based on experimental evidence of their

activity/function on a certain protein of interest, and then tested with validation sets. The accuracy of each model depends on the number of compounds used to create it and can be estimated by the correlation coefficient (R^2) and root mean squared error (RMSE), where a higher R^2 and low RMSE indicate higher model accuracy. The QSAR model with the highest specificity, sensitivity, accuracy, and the Matthews Correlation Coefficient was selected in MetaDrug for each particular activity or toxicity tested. The prediction of a therapeutic activity or toxic effect is calculated based on the ChemTree ability to correlate structural descriptors to that property using the recursive partitioning algorithm. The ChemTree parameters that gave the best results were as follows: path length 5, max segments 3, p value threshold Bonnferoni 0.99, p value multiway split 0.99 and number of random trees 50. The training set used in MetaCore/MetaDrug includes molecules that possess the property (positives) and chemicals that do not have such property (negatives) in approximately equal numbers. The marketed drugs were used if their number was greater than 100 in the disease QSAR models; drug candidates in clinical trials and preclinical compounds with in vivo activity have been added to the training set. The drugs that have been annotated to cause a particular toxic effect were used for the prediction of toxic effects.

Results and discussion

The antiproliferative capacity of ellipticine and its derivatives were characterized using in vitro MTT assay against four human tumor cell lines of gynecological origin (Table 1). Calculated IC_{50} values showed that ellipticine exhibited more pronounced action compared to the reference agent, cisplatin. The alkyl substituted analogs (Z-1 and Z-2) elicited substantially higher efficacy than parental Ellipticin against all of the utilized cell lines, followed by Z-6 while the other congeners proved to be roughly equipotent (Z-4 and Z-5) or less active when compared to the natural alkaloid. Ellipticine and its derivatives are aromatic compounds with intercalating properties and used as anticancer agents. The cytotoxicity of these compounds is due to their effect on the topoisomerase II enzyme as well as the hydroxyl group present in the 9 position of the pyridocarbazole ring in their structure (Fig. 1). The OH group in the ellipticine derivatives allows binding of the molecules to the major groove on DNA and stabilize the triple complex by hydrogen bonding with the enzyme (Fosse et al. 1992).

Table 1 The IC_{50} values determined from cytotoxicity assays

Compounds	Calculated IC_{50} values (μM)			
	HeLa	SiHa	MCF-7	MDA-MB-231
E	3.13	2.06	2.46	2.30
Z-1	0.06	0.63	0.91	0.77
Z-2	0.09	0.46	0.42	0.34
Z-4	54.39	19.21	4.33	27.09
Z-5	3.68	8.53	3.63	3.57
Z-6	2.42	4.92	1.72	2.99
Cisplatin	12.43	7.84	5.78	19.13

Given that vast majority of compounds, covering a number of ellipticine derivatives effective on tumor cells were reported to exert their effects through interfering with topoisomerase II reactions we screened the activities of the derivatives against DNA topoisomerase II reactions (Senarisoy et al. 2013; Ashley and Osheroff 2014; Miller et al. 2012; McClendon and Osheroff 2007). We therefore employed decatenatiation, intercalation, and cleavage assays. Decatenation assay is specific for topoisomerase II activity. It is based on the detection of kinetoplast DNA, the mitochondrial DNA of Crithidia fasciculata found as a catenated network of DNA rings (Senarisoy et al. 2013). All of the derivatives, Z-1, Z-2, Z-5, and Z-6, inhibited decatenation activity of topoisomerase II at 0.2 mM concentration. Among the compounds, Z-1 and Z-6 (Fig. 2, lanes 5 and 17, respectively), and Z-2 (Fig. 2, lane 8) partially retained inhibition at 0.1 mM concentration. Z-1 was found to be the most effective one in repeated densitometric analyses by revealing an avarage IC_{50} of 16 μM. On the other hand Z-2 and Z-6 gave rise to average IC_{50} values of 30 and 20 μM, respectively while Z-4 and Z-5 were relatively less effective as the interference caused by these compounds were not detectable upon dilution. Further dilutions revealed disappearance of the interference on decatenations (Fig. 2, lanes 6, 9, 12, 15 and 18 for Z1, Z3, Z4, Z5, and Z6, respectively). These results correlated with supercoil relaxing activity of DNA topoisomerase II using supercoiled plasmid DNA substrate, pBR322 (data not shown).

Although decatenation assay is a reliable method to investigate the effect of a given compound on human topoisomerase II, it is not solely informative about their mode of action. We next determined if the detected activities of the compounds were because of the formation of DNA strand breaks. We incubated the pBR322 and the alfa and beta isoforms of the enzyme in the presence of test compounds and terminated the reactions using SDS and then monitored DNA breaks following Proteinase-K treatment. Figure 3 shows a representative result obtained with the compounds and the control agents, Etoposide and mAMSA with both topoisomerase IIα and β isoforms (Fig. 3 upper and lower panels, respectively). Supercoiled pBR322 substrate (Fig. 3, upper and lower panels lane 1) was partially relaxed with topoisomerase IIα (Fig. 3, upper

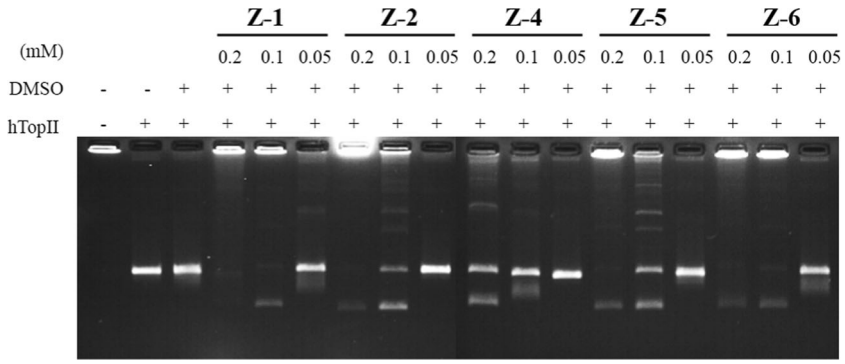

Fig. 2 Representative Topoisomerase II alfa decatenation assay in the presence of test compounds. Agarose gel photograph indicates the effect of the compounds Z-1, -2, -4, -5 and -6 on decatenation activity of human topoisomerase II. Lane 1, kDNA; lane 2, kDNA with 1 u topo II; lane 3, the same as lane 2 in the presence of DMSO, lanes 4–6, decatenation assays in the presence of 0.2, 0.1 and 0.05 mM Z1, respectively. The other test compounds, Z2 (lanes 7–9), Z4 (lanes 10–12), Z5 (lanes 13–15) and Z6 (lanes 16–18) were assessed at the same concentrations

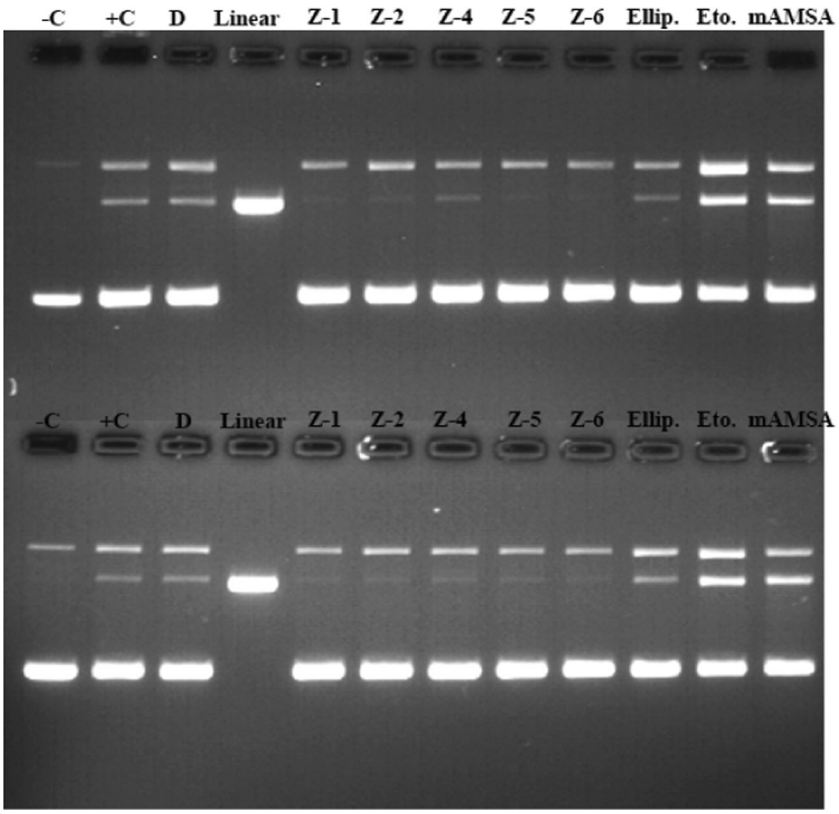

Fig. 3 A representative DNA strand break assay in the absence or the presence of test compunds. The assays were carried out either with human topoisomerase IIα (upper panel) or β (lower panel) isoform. The numbers correspond to Z-1, Z-2, Z-4, Z-5, and Z-6, respectively. See text for detailed description of applications

panel, lane 2) and β (Fig. 3, lower panel, lane 2) without an effect caused by DMSO (Fig. 3, upper and lower panels lane 3). None of the compounds (Fig. 3, upper and lower panels lanes 5, 6, 7, 8 and 9 for MK-1, -2, -4, -5 and -6, respectively) and parental ellipticine (Fig. 3, upper and lower panels lane 10) gave rise to a double strand breakage pattern with the method we employed while both Etoposide and mAMSA gave rise to linear DNA bands (Fig. 3, upper and lower panels lanes 11 and 12) with a migration patter similar linearized pBR322 (Fig. 3, upper and lower panels lane 4).

We, then, investigated the intercalative potential of the compounds through the shift of DNA bands from relaxed to negatively supercoiled DNA populations. As seen in Fig. 4, the test compounds Z1 and Z6 showed a remarkable intercalation (Fig. 4. Lanes 3 and 7, respectively) somewhat similar to the intercalation of Etd-Br (Fig. 4, lane 8). The band shifting patterns for Z2, Z4, and Z5 were neglectable

as they were comparable with relaxed pBR322 (Fig. 4, lane 1) with human topoisomerase II (Fig. 4, lane 2).

We next used in silico simulations for five molecules using Glide/IFD, Glide/QPLD, Glide/SP, and Glide/XP docking protocols. Four standard inhibitors were also studied for comparison. Table 2 shows top docking scores of the test compounds at the binding pocket of human DNA topoisomerase II alpha. Different docking algorithms were used in docking simulations. Although GOLD Fitness and ChemScore functions were not able to distinguish the docking scores significantly between the studied molecules as well as ellipticine, molecules had similar binding interactions with ellipticine and they have better fitness scores compared with positive control. Glide/SP and XP scoring functions did not result in dramatic scoring difference within the compounds set and reference molecules. However, all docking algorithms showed that the molecules have similar or better docking scores than reference molecules. Higher docking scores of compound Z-1 compared with reference molecules were observed in IFD and QPLD docking. It's known that both IFD and QPLD have better performances compared with Glide/SP and XP modules. An induced fit protocol is used to assist with increasing the flexibility of atoms of the target protein at the active site and thus accurately locates the ligand with a reasonable orientation. Successful docking approaches require the accurate calculations and modeling of the partial atomic charges that ligand is bearing. Quantum mechanics (QM) modeling may give the highest level of docking precision when specifically, the induced charge polarization of the binding pocket residues was considered. For the underlying consideration regarding accuracy of docking results, QPLD, based on ab initio charge calculations was used. The 2D and 3D ligand interaction diagrams of Z-1 at the binding site. Crucial amino acids were found as Glu461, Gly462, Asp463, Leu486, Arg487, Gly488, Tyr757, His759, Gly760, Glu761, Met762, Ser763, Leu764, and Met766. When Z1, Z4, and Z5 docking poses were compared, it can be seen that bioactive conformation of Z1 is totally different than Z4 and Z5 (Fig. S1, Supporting Materials).

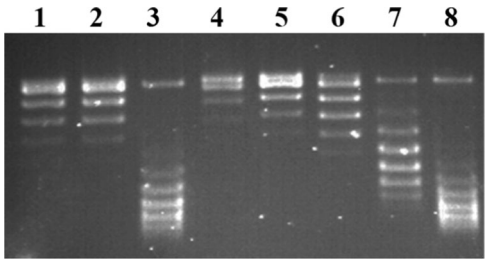

Fig. 4 DNA intercalation assay. Intercalation by ellipticine derivatives was based on the detection of the band shift from relaxed to negatively supercoiled DNA. Assays that contained only the relaxed DNA substrate or relaxed DNA and topoisomerase I with no compound are shown in lanes 1 and 2, respectively. The derivatives Z-1, Z-2, Z-4, Z-5, and Z-6 are applied on the lanes 3–7, respectively. Strong intercalator agent, Et-Br is shown at the lane 8

MD simulations were performed for Z1 and ellipticine to see the structural and dynamical profiles throughout the simulations. (Figs. S2, S3, Supporting Materials). RMSD and RMSF plots were compared for Z1 and ellipticine in Fig. S2. Binding interactions analyses of Z1 showed that especially two residues Met762 and Met766 are crucial for ligand-target interactions.

Pharmacokinetic profiles of studied molecules Z-1, Z-2, and Z-6 were also performed by binary QSAR models of MetaCore/MetaDrug platform. Results showed that within 26 toxicity QSAR models, Z-1 and Z-2 showed toxicity in only three models (AMES, Anemia, and cardiotoxicity). Compound Z-6 showed toxicity profile only in four models (AMES, Anemia and liver cholestasis and neurotoxicity). However, it must be noted that three out of four results of toxic profiles in compound Z6 were in near threshold (0.5). Toxicity predictions were also compared with known

Table 2 Docking scores of the test compounds (kcal/mol)

Compounds	IFD Docking score	QPLD Docking score	Glide/XP Docking score	Glide/SP Docking score	GOLD Docking score	
					Fitness score	Chem score (kcal/mol)
Z-1	−12.378	−7.428	−4.766	−7.344	41.21	−5.22
Z-2	−12.337	−6.917	−5.888	−6.911	45.38	−6.14
Z-4	−11.616	−7.208	−4.491	−7.025	41.85	−5.18
Z-5	−12.521	−7.288	−5.860	−7.043	46.12	−5.21
Z-6	−12.306	−7.061	−6.293	−7.345	43.60	−4.71
Ellipticine	−8.901	−6.952	−6.428	−8.420	34.54	−5.38
Ciprofloxacin	−6.246	−6.431	−6.467	−6.680	NA	NA
Ofloxacin	−6.358	−6.523	−4.909	−7.140	NA	NA
Mitonafide	−5.107	−5.893	−5.010	−6.450	NA	NA

inhibitor ellipticine. Ellipticine showed toxicity in five models (AMES, carcinogenicity in male mouse, carcinogenicity in rat female, cardiotoxicity, and genotoxicity) out of 26 different toxicity QSAR models (Table S1, Supporting Materials).

Taken together, our results showed that the compounds Z1, Z2, and Z6 have significant potential as compounds targeting human DNA topoisomerase II. Given that the alfa and beta isoforms of human DNA topoisomerase II is expressed in a different pattern in normal and cancer cells, differentiating between these two isoforms is an important aspect of topoisomerase-targeting drug development. However, the absence of DNA breaks in either isoform when compared to the reference compounds revealed that ellipticine derivatives could affect inhibition of catalytic activity rather than stabilizing the covalent complex.

Data accessibility

The datasets supporting this study have been uploaded as part of the electronic supplementary material.

Acknowledgements This study is supported by the grant of TUBITAK 115Z349 (PI; ZT).

Author contributions MK, enzyme assays; VA, synthesis and characterization of test compounds; AK and IZ, mammalian cell viability assays; MZ and KS, in silico analyses; SD, in silico analyses and editing manuscript; HO, consultation and data analyses; YE, designing experiments, synthesis and characterization of test compounds, interpretation of data; SZ, designing experiments, enzyme assays, editing the manuscript; ZT, designed the project, enzyme assays, interpretation of data and writing manuscript.

Compliance with ethical standards

Conflict of interest The authors declare that they have no conflict of interest.

Publisher's note Springer Nature remains neutral with regard to jurisdictional claims in published maps and institutional affiliations.

References

Ashley RE, Osheroff N (2014) Natural products as topoisomerase II poisons: effects of thymoquinone on DNA cleavage mediated by human topoisomerase IIα. Chem Res Toxicol 27:787–793

Champoux JJ (2001) DNA topoisomerases: structure, function, and mechanism. Annu Rev Biochem 70:369–413

Chikamori K, Grozav AG, Kozuki T, Grabowski D, Ganapathi R, Ganapathi MK (2010) DNA topoisomerase II enzymes as molecular targets for cancer chemotherapy. Curr Cancer Drug Tar 10:758–777

Coban G, Zencir S, Zupkó I, Réthy B, Gunes HS, Topcu Z (2008) Synthesis and biological activity evaluation of 1H-benzimidazoles via mammalian DNA topoisomerase I and cytostaticity assays. Eur J Med Chem 44:2280–2285

Deane FM, O'Sullivan EC, Maguire AR, Gilbert J, Sakoff JA, McCluskey A, McCarthy FO (2013) Synthesis and evaluation of novel ellipticines as potential anti-cancer agents. Org Biomol Chem 1:1334–1344

Delgado JL, Hsieh CM, Chan NL, Hiasa H (2018) Topoisomerases as anticancer targets. Biochem J 475:373–398

Desmond molecular dynamics system, D.E.S.R., New York, NY, 2017.

Fosse P, Rene B, Charra M, Paoletti C, Saucier J (1992) Stimulation of topoisomerase II-mediated DNA cleavage by ellipticine derivatives structure–activity relationship. Mol Pharm 42:590–595

Friesner R, Banks JL, Murphy RB, Halgren TA, Klicic JJ, Mainz DT, Repasky MP, Knoll EH, Shelley M, Perry JK, Shaw DE, Francis P (2004) Glide: a new approach for rapid, accurate docking and scoring. 1. Method and assessment of docking accuracy. J Med Chem 47:1739–1749

Garbett NC, Graves DE (2004) Extending nature's leads: the anticancer agent ellipticine. Curr Med Chem Anticancer Agents 4:149–172

Gul HI, Cizmecioglu M, Zencir S, Gul M, Canturk P, Atalay M, Topcu Z (2009) Cytotoxic activity of 4'-hydroxychalcone derivatives against Jurkat cells and their effects on mammalian DNA topoisomerase I. J Enzym Inhib Med Chem 24:804–807

Hoover WG (1985) Canonical dynamics: equilibrium phase-space distributions. Phys Rev A 31:1695–1697

Iacopetta D, Rosano C, Puoci F, Parisi OI, Saturnino C, Caruso A et al. (2017) Multifaceted properties of 1,4dimethylcarbazoles: focus on trimethoxybenzamide and trimethoxyphenylurea derivatives as novel human topoisomerase II inhibitors. Eur J Pharm Sci 96:263–272

Ketron AC, Osheroff N (2014) Phytochemicals as anticancer and chemopreventive topoisomerase II poisons. Phytochem Rev 13:19–35

Kuo PL, Hsu YL, Chang CH, Lin CC (2005) The mechanism of ellipticine-induced apoptosis and cell cycle arrest in human breast MCF-7 cancer cells. Cancer Lett 223:293–301

Lichota A, Gwozdzinski K (2018) Anticancer activity of natural compounds from plant and marine environment. Int J Mol Sci 19:1–38

Martyna GJ (1994) Remarks on "Constant-temperature molecular dynamics with momentum conservation". Phys Rev E 50:3234–3236

McClendon AK, Osheroff N (2007) DNA topoisomerase II, genotoxicity, and cancer. Mutat Res 623:83–97

Metacore/Metadrug platform, Clarivate Analytics (2019) https://portal.genego.com/

Miller CM, O'Sullivan EC, Devine KJ, McCarthy. CM (2012) Synthesis and biological evaluation of novel isoellipticine derivatives and salt. Org Biomol Chem 10:7912–7921

Moody DL, Dyba M, Kosakowska-Cholody T, Tarasova NI, Michejda CJ (2007) Synthesis and biological activity of 5-aza-ellipticine derivatives. Bioorg Med Chem Lett 17:2380–2384

Mosmann T (1983) Rapid colorimetric assay for cellular growth and survival: application to proliferation and cytotoxicity assays. J Immunol Methods 65:55–63

Rouëssé J, Spielmann M, Turpin F, Le Chevalier T, Azab M, Mondésir JM (1993) Phase II study of elliptinium acetate salvage treatment of advanced breast cancer. Eur J Cancer 29:856–859

Senarisoy M, Canturk P, Zencir S, Baran Y, Topcu Z (2013) Gossypol interferes with both type I and type II topoisomerase activities without generating strand breaks. Cell Biochem Biophys 66:199–204

Thompson D, Miller C, McCarthy FO (2008) Computer simulations reveal a novel nucleotide-type binding orientation for ellipticine-based anticancer c-kit kinase inhibitors. Biochemistry 47:10333–10344

Topcu Z (2001) DNA topoisomerases as targets for anticancer drugs. J Clin Pharm Ther 26:405–416

Topcu Z, Ozturk B, Kucukoglu O, Kilic E (2008) Inhibition of mammalian type I DNA topoisomerase by Helichrysum pamphylicum is correlated with the total antioxidant capacities of its individual flavonoids. Z Naturforsch C 63:69–74

Vann KR, Ekiz G, Zencir S, Bedir E, Topcu Z, Osheroff N (2016a) Effects of secondary metabolites from the fungus Septofusidium berolinense on DNA cleavage mediated by human topoisomerase IIα. Chem Res Toxicol 29:415–420

Vann KR, Ergun Y, Zencir S, Oncuoglu S, Osheroff N, Topcu Z (2016b) Inhibition of human DNA topoisomerase IIα by two novel ellipticine derivatives. Bioorg Med Chem Lett 26:1809–1812

Verdonk ML, Cole JC, Hartshorn MJ, Murray CW, Taylor RD (2003) Improved protein-ligand docking using GOLD. Proteins 52:609–623

Wang JC (1971) Interaction between DNA and an *Escherichia coli* protein omega. J Mol Biol 55:523–533

Wendorff TJ, Schmidt BH, Heslop P, Austin CA, Berger JM (2012) The structure of DNA-bound human topoisomerase II alpha: conformational mechanisms for coordinating inter-subunit interactions with DNA cleavage. J Mol Biol 424:109–124

Zupkó I, Molnár J, Réthy B, Minorics R, Frank E, Wölfling J et al. (2014) Anticancer and multidrug resistance-reversal effects of solanidine analogs synthetized from pregnadienolone acetate. Molecules 17:2061–2076